THE ASTROPHYSICAL JOURNAL, 506:485–494, 1998 October 20

STRUCTURE FORMATION WITH GENERALIZED DARK MATTER

WAYNE HU[1]
Institute for Advanced Study, Princeton, NJ 08540
Received 1998 January 26; accepted 1998 June 1

ABSTRACT

The next generation of cosmic microwave background (CMB) experiments, galaxy surveys, and high-redshift observations can potentially determine the nature of the dark matter observationally. With this in mind, we introduce a phenomenological model for a generalized dark matter (GDM) component and discuss its effect on large-scale structure and CMB anisotropies. Specifying the gravitational influence of the otherwise noninteracting GDM requires not merely a model for its equation of state but one for its full stress tensor. From consideration of symmetries, conservation laws, and gauge invariance, we construct a simple but powerful three-component parameterization of these stresses that exposes the new phenomena produced by GDM. Limiting cases include: a particle component (e.g., weakly interacting massive particles, radiation, or massive neutrinos), a cosmological constant, and a scalar field component. Intermediate cases illustrate how the clustering properties of the dark matter can be specified independently of its equation of state. This freedom allows one to alter the amplitude and features in the matter-power spectrum relative to those of the CMB anisotropies while leaving the background cosmology fixed. Conversely, observational constraints on such phenomena can help determine the nature of the dark matter.

Subject headings: cosmic microwave background — cosmology: theory — dark matter — large-scale structure of the universe

1. INTRODUCTION

Upcoming cosmic microwave background (CMB) missions, galaxy redshift surveys, and high-redshift observations will produce such a wealth of high-quality data that even the extended cold dark matter (CDM) model with 11 free parameters (e.g., Jungman et al. 1996) may fail to fit them. One must face the very real possibility that none of our current ab initio models will survive the upcoming confrontation with the data.

How might one generalize the CDM model? The cornerstone of all modern cosmologies is, and will likely remain, gravitational instability in a world model that is homogeneous and isotropic on the large scale (e.g., Peebles et al. 1991). Models for the dark matter sector, on the other hand, are presently limited by the number of candidates that are considered well-motivated from the particle physics standpoint, e.g., weakly interacting massive particles (CDM), massive neutrinos, scalar fields (see Coble, Dodelson, & Frieman 1996; Ferreira & Joyce 1997; Caldwell, Dave & Steinhardt 1998, for recent assessments), and topological defects (Spergel & Pen 1997). If none of these candidates survive the confrontation with high-precision cosmological measurements, we will be forced to solve the inverse problem: can one determine the nature of the dark matter and reconstruct the model for structure formation directly from the observations?

Explorations of the dark matter sector have been undertaken recently by Turner & White (1997) and Caldwell et al. (1998), who considered dark matter with an arbitrary equation of state that possesses no fluctuations and scalar-field type fluctuations, respectively. The former case does not present a complete theory of structure formation, as it can only apply below the horizon at any given time for adiabatic models. The latter case provides an interesting example of an exotic dark matter component but does not exhaust the possibilities for its gravitational properties. For example, a hot dark matter component has an equation of state like matter today but clusters only up to a finite scale. This scale is substantially below the current horizon scale, where it would be for the analogous scalar field model (Ferreira & Joyce 1997).

Starting from the general principles of symmetry, energy-momentum conservation and gauge invariance, we build in § 2 a phenomenological parameterization of the dark matter that includes all of the currently popular dark matter theories as special cases. The main result is the link established between the clustering properties of the dark matter and the model for its underlying stresses. Importantly, these properties are not determined by the background equation of state in the general case. Through their effect on the growth rate of perturbations, discussed in § 3, these clustering properties manifest themselves as independent features in the power spectra of large-scale structure and CMB anisotropies as discussed in § 4 and § 5. We summarize the main results in § 6 and present a short Appendix that highlights the scalar field case.

2. DARK MATTER PROPERTIES

2.1. *General Principles*

The gravitational influence of an arbitrary dark matter component is controlled by its stress-energy tensor $T_{\mu\nu}(\boldsymbol{x}, \eta)$, where $\eta = \int dt/a$ is the conformal time with $a(t)$ as the scale factor normalized to unity today. In general, the symmetric four-tensor $T_{\mu\nu}$ has ten components that can be divided into four classes: the energy density ρ_g (1), the isotropic stress or pressure p_g (2), the momentum density $(\rho_g + p_g)v_g^i$ (3), and the anisotropic stress $p_g\pi_g^{ij}$ (4). The five components of the

[1] Alfred P. Sloan Fellow.

anisotropic stress can be further separated by their transformation properties under rotations into a scalar component (1), vector components (2), and tensor components (2). Since only scalar components exhibit gravitational instability, we hereafter neglect the vector and tensor contributions.[2] Energy-momentum conservation $T^{;\nu}_{\mu\nu} = 0$ introduces four constraints, leaving only two independent parameters for the dark matter. One can choose these to be the pressure p_g and scalar anisotropic stress amplitude π_g (see Bardeen 1980, eq. [2.18]) without loss of generality.

The isotropy of the background implies that the anisotropic stress and momentum density can only be present as a perturbation. The conservation laws then reduce to a single relation,

$$\frac{\dot{\rho}_g}{\rho_g} = -3(1 + w_g)\frac{\dot{a}}{a}, \tag{1}$$

where overdots represent conformal time derivatives and $w_g = p_g/\rho_g$. Likewise the Einstein equations $G_{\mu\nu} = 8\pi G T_{\mu\nu}$ reduce to

$$\left(\frac{\dot{a}}{a}\right)^2 = \frac{8\pi G}{3} a^2 \sum_i \rho_i - K, \tag{2}$$

where the sum is over the density contributions of all matter species and the background curvature is $K = -H_0(1 - \Omega_{\rm tot})$ with $\Omega_{\rm tot} = \sum_i \Omega_i$. As usual, the expansion rate today is given by the Hubble constant $H_0 \equiv (\dot{a}/a)_{a=1} = 100\ h$ km s^{-1} Mpc^{-1}, to which each species contributes according to its fraction of the critical density $\Omega_i = 8\pi G\rho_i/3H_0^2$.

The background evolution is thus completely specified by the equation of state $w_g(a)$. This is *not* true of the perturbations, where we are left with the freedom to specify δp_g and π_g. It is convenient to separate out the nonadiabatic stress or entropy contribution

$$p_g \Gamma_g = \delta p_g - c_g^2 \delta\rho_g, \tag{3}$$

where the adiabatic sound speed is

$$c_g^2 = \frac{\dot{p}_g}{\dot{\rho}_g} = w_g - \frac{1}{3}\frac{\dot{w}_g}{1 + w_g}\left(\frac{\dot{a}}{a}\right)^{-1}. \tag{4}$$

Therefore, $p_g = w_g \rho_g$ does *not* imply $\delta p_g = w_g \delta\rho_g$ (due to temporal or spatial variations in w_g) and, furthermore, if $\Gamma_g \neq 0$, the function $w_g(a)$ does not completely specify the pressure fluctuation.

In the following, we adopt the notation of Hu et al. (1998b). For brevity, we present only the aspects of perturbation theory that are altered by the presence of generalized dark matter (GDM). Energy-momentum conservation yields the continuity equation for the density fluctuation $\delta_g \equiv \delta\rho_g/\rho_g$,

$$\left(\frac{\delta_g}{1 + w_g}\right)^{\cdot} = -(kv_g + 3\dot{h}_\delta) - 3\frac{\dot{a}}{a}\frac{w_g}{1 + w_g}\Gamma_g, \tag{5}$$

and the Euler equation

$$\dot{v}_g = -\frac{\dot{a}}{a}(1 - 3c_g^2)v_g + \frac{c_g^2}{1 + w_g} k\delta_g + \frac{w_g}{1 + w_g} k\Gamma_g - \frac{2}{3}\frac{w_g}{1 + w_g}\left(1 - \frac{3K}{k^2}\right)k\pi_g + kh_v. \tag{6}$$

The metric sources h_δ and h_v depend on the choice of gauge and are

$$h_\delta = \begin{cases} h_L & \text{Synchronous}, \\ \Phi & \text{Newtonian}, \end{cases}$$
$$h_v = \begin{cases} 0 & \text{Synchronous}, \\ \Psi & \text{Newtonian}. \end{cases} \tag{7}$$

Note that $h_L = h/6$ in the notation of Ma & Bertschinger (1995). Seed perturbations (e.g., defects) whose total contribution is first order in the perturbations can also be modeled in this manner by rewriting equations (1), (5), and (6) in terms of $\delta\rho_g$ and $(p_g + \rho_g)v_g$ instead of the relative perturbations (see eq. [A9]).

2.2. *Stress Model*

Up to this point, we have made no assumptions whatsoever about the nature of the dark matter, since w_g, Γ_g, and π_g have been left as free functions. We now need to parameterize these functions. Dark matter with $w_g < 0$ is favored by current observational constraints, such as the combination of the ages of globular clusters and the high Hubble constant measurements (Chiba, Sugiyama, & Nakamura 1997; Caldwell et al. 1998), as well as supernova luminosity distance measures (Perlmutter et al. 1998; Riess et al. 1998). If $w_g < 0$ and is slowly varying compared with the expansion rate $(\dot{a}/a)$ such that $c_g^2 < 0$, the adiabatic pressure fluctuation produces accelerated collapse rather than support for the density perturbation. In a GDM-dominated universe, perturbations would rapidly go nonlinear once the sound horizon has been crossed, $|k\int c_g\, d\eta| > 1$. This situation is unacceptable for a model of structure formation.

In this $w_g < 0$ regime, it is interesting to consider whether nonadiabatic pressure can act to stabilize the perturbation. This requires a relation of the type $w_g \Gamma_g \propto \delta_g$. One is not, however, allowed complete freedom in establishing this relation. Adiabatic pressure, density, and velocity perturbations are gauge dependent, whereas nonadiabatic pressure perturbations are not. Therefore, stabilization in one frame of reference does not equate to stabilization in another. One should avoid having the properties of the GDM depend on an arbitrary choice of frame and hence unphysically on the perturbations in the other species. This requirement can be achieved by defining the relation in the rest frame of the GDM where $T_i^0 = 0$,

$$w_g \Gamma_g = (c_{\rm eff}^2 - c_g^2)\delta_g^{\rm (rest)}. \tag{8}$$

We further assume the effective sound speed $c_{\rm eff}^2$ is only a function of time. If $c_{\rm eff}^2 > 0$, pressure support is obtained. The gauge transformation into an arbitrary frame gives

$$\delta_g^{\rm (rest)} = \delta_g + 3\frac{\dot{a}}{a}(1 + w_g)\frac{(v_g - B)}{k}, \tag{9}$$

yielding a manifestly gauge-invariant form for the nonadiabatic stress (see Bardeen 1980; Kodama & Sasaki

[2] Vector and tensor contributions do, however, affect CMB anisotropies and can act as additional degrees of freedom when normalizing large-scale structure to CMB measurements (e.g., Caldwell & Steinhardt 1998).

1984). Here B represents the time-space component of metric fluctuations and vanishes in both the synchronous and Newtonian gauges. The Euler equation can then be rewritten as

$$\dot{v}_g = -\frac{\dot{a}}{a} v_g + \frac{c_{\rm eff}^2}{1+w_g} k\delta_g^{(\rm rest)} - \frac{2}{3}\frac{w_g}{1+w_g} k\left(1-\frac{3K}{k^2}\right)\pi_g + kh_v \,. \quad (10)$$

Thus $c_{\rm eff}^2$ may be thought of as a rest frame sound speed. By inspection of equations (10) and (5), we determine that the critical scale for stabilization is the effective sound horizon,

$$s_{\rm eff} = \int d\eta c_{\rm eff} \,. \quad (11)$$

This assumes w_g is not varying at a rate much greater than the expansion rate (see the Appendix).

The anisotropic stress can also affect the density perturbations. A familiar example is that of fluid, where it represents viscosity and damps density perturbations. More generally, the anisotropic stress component is the amplitude of a three tensor that is linear in the perturbation. A natural choice for its source is kv_g, the amplitude of the velocity shear tensor $\partial^i v_g^j$. However, it must also be gauge invariant and generated by the corresponding shear term in the metric fluctuation H_T. The relationship between velocity/metric shear and anisotropic stress may be parameterized with a "viscosity parameter" $c_{\rm vis}^2$,

$$w_g\left(\dot{\pi}_g + 3\frac{\dot{a}}{a}\pi_g\right) = 4c_{\rm vis}^2(kv_g - \dot{H}_T) \quad (12)$$

where in the Newtonian gauge $H_T = 0$ and in the synchronous gauge $H_T = h_T(= -h/2 - 3\eta$; Ma & Bertschinger 1995). The specific form of this equation is designed to recover the free-streaming equations of motion for radiation with an approximate closing of the angular moment hierarchy at the quadrupole (Hu et al. 1995). The physical interpretation of equation (12) is that the anisotropic stress will act to damp out velocity fluctuations on shear-free frames ($H_T = 0$) if $c_{\rm vis}^2 > 0$. We call $s_{\rm vis} = \int c_{\rm vis}\, d\eta$ the viscous scale.

We shall see in the following sections that this parameterization captures many of the essential features of GDM as it corresponds to a means of altering its clustering properties. In the limit that $(w_g, c_{\rm eff}^2, c_{\rm vis}^2) \to (w_g, 1, 0)$, scalar-field dark matter is recovered exactly (see the Appendix). CDM is similarly recovered with (0, 0, 0), radiation can be modeled as $(\frac{1}{3}, \frac{1}{3}, \frac{1}{3})$, and hot dark matter (HDM) or warm dark matter is modeled in a similar matter described in § 4.3.

Cases that this *Ansatz* does *not* cover involve mainly models in which stress fluctuations are not derived from density and velocity perturbations and so act as external sources for the perturbations. This situation occurs in the case of nonlinear seed perturbations (see Hu, Spergel, & White 1997 for a parallel treatment). Note that in such models both vector and tensor stresses must also be modeled to yield a complete theory for structure formation (see Hu & White 1997b; Turok, Pen, & Seljak 1997).

Equations (5), (8), and (10) can now be introduced into any of the standard codes that solve the Einstein-Boltzmann equations. We employ the code of Hu et al. (1995) for the examples below. We furthermore show adiabatic models for illustrative purposes, but of course isocurvature models can be similarly obtained through a change in the initial conditions.

3. PERTURBATION GROWTH

By introducing a means by which fluctuations in the GDM are stabilized, we change the growth rate of fluctuations in the baryons and any CDM that may be present. The clustering properties of the GDM thus have consequences for both large-scale structure and CMB anisotropies, as we shall see in §§ 4 and 5. Here we summarize results for the growth rate of perturbations proved in Hu & Eisenstein (1998).

3.1. *Above the Sound Horizon*

Above the stabilization scale of all species and in the absence of background curvature ($K = 0$), perturbations evolve so as to keep the Newtonian curvature Φ and potential Ψ constant

$$(k^2 - 3K)\Phi = 4\pi G a^2 \sum_i \rho_i \delta_i^{(\rm rest)} \,,$$
$$k^2(\Psi + \Phi) = -8\pi G a^2 \sum_i p_i \pi_i \,, \quad (13)$$

except during periods when the dominant equation of state w changes. Here the potentials vary mildly such that (Bardeen 1980)

$$\Phi - \frac{2}{3}\frac{1}{1+w}\Psi = \text{const} \,. \quad (14)$$

For reference, dominance of GDM relative to matter occurs at

$$a_g = \left(\frac{\Omega_g}{\Omega_m}\right)^{1/3w_g} \,. \quad (15)$$

The result is that, during periods when the equation of state is slowly varying, the total density fluctuation $\delta^{(\rm rest)} = \sum \delta_i^{(\rm rest)}\rho_i / \sum \rho_i$ grows as

$$\delta^{(\rm rest)} \propto a^{1+3w} \,. \quad (16)$$

We display an example of this large-scale evolution in Figure 1.

Since CMB anisotropies are only dependent on the time evolution of the potentials, the effect of GDM here is very weak. The exception is the $w_g \to -1$ limit, where the potentials decay to zero and the cosmological constant case is recovered. Note, however, that a curvature term in the background and a dark matter component with $w_g = -\frac{1}{3}$ give identical contributions to the expansion rate but are not similar in their contribution to large-angle CMB anisotropies.

Finally, the division of density fluctuations between the GDM and the matter components, i.e., δ_g/δ_m, depends on the form of the GDM stress. This is because of the appearance of the nonadiabatic stress term in the continuity equation (5) that relates the density and metric fluctuations. As $c_{\rm eff}^2$ increases, δ_g/δ_m decreases. This affects the amplitude of the matter-power spectrum as we shall see (§ 4.1).

3.2. *Below the Sound Horizon*

Below the effective sound horizon of the GDM its perturbations stabilize. If GDM dominates the energy density,

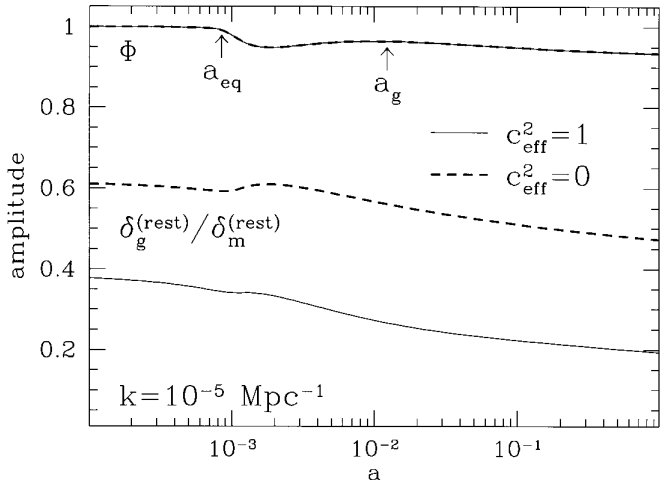

FIG. 1.—Large-scale perturbation evolution ($ks_{\rm eff} \gg 1$) with GDM of $w_g = -\frac{1}{6}$, $c^2_{\rm eff} = 1$ (*solid line*; scalar fields) and 0 (*dashed line*; stress-gradient free). The Newtonian curvature Φ is independent of $c^2_{\rm eff}$ and varies only when the background equation of state changes at $a_{\rm eq}$ and a_g. However, the ratio of density perturbations in the GDM and matter depends on $c^2_{\rm eff}$. The cosmological parameters here are $\Omega_{\rm tot} = 1$, $\Omega_g = 0.9$, $\Omega_b h^2 = 0.0125$, and $h = 0.7$.

$\delta_g^{(\rm rest)}$ oscillates with a decaying amplitude of

$$A \propto a^{(-1+3w_g)/2} c_{\rm eff}^{-1/2} \tag{17}$$

and rapidly becomes a smooth density component compared with the fluctuations in the other species. We display a case where there is also a non-negligible CDM component in Figure 2. Once GDM dominates the energy density of the universe at a_g, then the smoothing of the GDM component will also slow or halt the growth in the matter species. In particular, the growth will slow to a halt if $w_g < 0$ and scale as a^p with $4p = (1 + 24\Omega_m/\Omega_{\rm tot})^{1/2} - 1$ if $w_g = 0$. Analytic solutions for how this process occurs are given in Hu & Eisenstein (1998).

The net effect is that if there is enough CDM to ensure that the universe was matter dominated sometime in the past, perturbation growth is suppressed by a scale-independent factor below the effective sound horizon $s_{\rm eff}$ at GDM domination. This suppression decreases until it disappears above $s_{\rm eff}$ today. For the CMB, the suppression of growth in the density perturbations causes the potentials to decay to zero, leading to a contribution potentially 36 times larger than the Sachs-Wolfe effect in the anisotropy power spectrum. We shall see in § 5.2 why this limiting value is never reached in practice.

On the other hand, if matter never dominated the expansion, as is the case if CDM is absent, even more dramatic effects occur. In this case, growth even for $c^2_{\rm eff} = 0$ is highly suppressed on small scales because of an extended period of radiation domination (assuming $w_g < 0$). The controlling scale is therefore the horizon at GDM-radiation equality

$$a_{g\rm eq} = \left(\frac{\Omega_r}{\Omega_g}\right)^{1/(1-3w_g)}, \tag{18}$$

i.e.,

$$k_{g\rm eq} = \left(\frac{\dot a}{a}\right)_{a=a_{g\rm eq}} = \sqrt{\frac{2}{\Omega_r}}\,\Omega_g H_0 \left(\frac{\Omega_r}{\Omega_g}\right)^{-3w_g/(1-3w_g)}. \tag{19}$$

Above this scale, perturbations grow as in equation (16); below this scale, perturbations only experience significant growth after GDM domination. Because GDM domination for $w_g < 0$ is delayed compared with an equivalent $w_g = 0$ universe, the critical scale is larger in such single component GDM models than in the CDM case.

3.3. *Viscosity*

Finally, the viscous stresses of equation (12) can dissipate fluctuations in the GDM. In Figure 3 we show an example with $w_g = \frac{1}{3}$ GDM replacing the three massless neutrinos in an otherwise standard CDM universe (sCDM; $\Omega_{\rm tot} = 1 \approx \Omega_m$, $h = 0.5$, $\Omega_b h^2 = 0.0125$). The real neutrino background radiation contains an anisotropic stress due to the quadrupole moment of its temperature distribution. Modeling the neutrinos as GDM allows us to explore the consequences of its anisotropy by varying $c^2_{\rm vis}$ and also illustrates

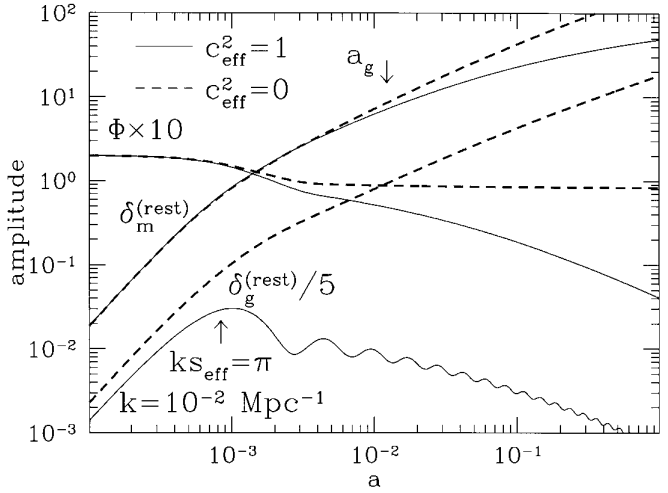

FIG. 2.—Small-scale perturbation evolution for the GDM and the matter density perturbations in the same models as Fig. 1 with $c^2_{\rm eff} = 1$ (*dashed lines*) and $c^2_{\rm eff} = 0$ (*solid lines*). GDM perturbations stabilize once $ks_{\rm eff} > \pi$ and their relative absence ($\delta_g^{(\rm rest)}/\delta_m^{(\rm rest)} \ll 1$) then slow the growth of matter perturbations once the expansion is also GDM dominated $a > a_g$ leaving the potential Φ to decay.

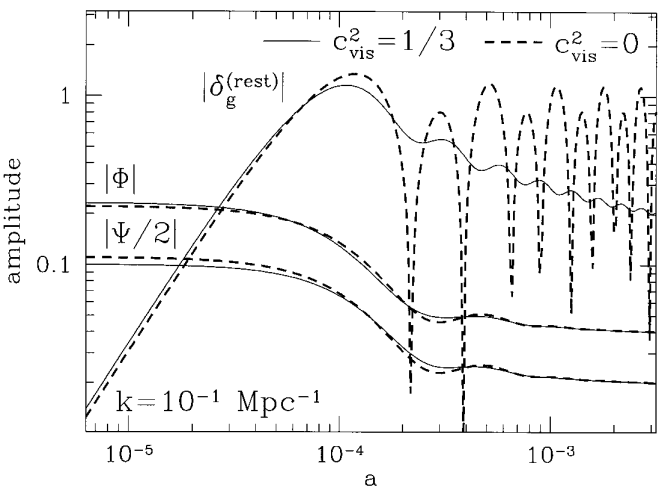

FIG. 3.—Viscous effects with GDM $w_g = \frac{1}{3}$ replacing the three species of massless neutrinos in the sCDM model ($\Omega_{\rm tot} = 1 \approx \Omega_m$, $h = 0.5, \Omega_b h^2 = 0.0125$). With the viscosity parameter set to mimic radiation $c^2_{\rm vis} = \frac{1}{3}$ (*solid lines*), the perturbations in the GDM decay, whereas with $c^2_{\rm vis} = 0$, they do not. This distinction has a negligible effect on the behavior of the potentials Φ and Ψ well after sound horizon crossing

the phenomenological manifestations of the viscosity parameter.

In the absence of anisotropic stresses (*dashed lines*; $c_{\rm vis}^2 = 0$), perturbations in the GDM oscillate. Changing $c_{\rm vis}^2$ to $\frac{1}{3}$ to approximate the radiative viscosity of the real neutrinos, the density perturbations damp once $ks_{\rm vis} \gtrsim \pi$. Note, however, its effect on the gravitational potentials Φ and Ψ well after crossing the sound horizon when the large-scale structure observed is negligible. This is because the pressure fluctuations are sufficiently effective to make the GDM perturbations smooth in comparison with the growing species (see Fig. 2). The extra smoothing due to viscous damping affects perturbations little.

The anisotropic stress does change the behavior of the potentials at early times because it enters directly in to the Poisson equations (13). We shall see in § 5.3 that correspondingly viscous effects are more important for the CMB than large-scale structure so long as $|c_{\rm eff}^2| > |c_{\rm vis}^2|$.

4. LARGE-SCALE STRUCTURE

The large-scale structure of the universe depends on the detailed properties of the GDM. The main result of this is that the clustering scale becomes independent of the equation of state of the dark matter. By changing the growth rate of perturbations, the clustering properties change the amplitude of and features in the matter power spectrum. Here we present concrete examples of this process that include scalar fields, radiation, and hot dark matter as special cases.

4.1. *Sound Horizon and Scalar Fields*

The introduction of a stabilization scale or effective sound horizon $s_{\rm eff}$ for the GDM places a feature in the matter power spectrum between that scale at GDM domination and today, i.e.,

$$s_{\rm eff}^{-1}(a = 1) < k < s_{\rm eff}^{-1}(a = a_g) \, . \tag{20}$$

The limiting cases are the scalar-field example, where the effective sound speed is the speed of light $c_{\rm eff}^2 = 1$, and the pressure-gradient free case with $c_{\rm eff}^2 = 0$. In Figure 4, we display the effect of varying $c_{\rm eff}^2$ on the power spectrum of the matter holding the background cosmology fixed. These models have been consistently normalized to the *COBE* CMB anisotropy measurement at large scales via the fitting form of Bunn & White (1997; their eqs. [17]–[20]).

The amplitude of fluctuations at the fiducial 8 h^{-1} Mpc scale, σ_8, is affected in three ways. The presence of a clustering scale reduces the growth rate below it, leading to a relative suppression of small-scale power. However, the absolute amplitude of large-scale fluctuations also changes with the clustering scale. As shown in the last section, decreasing $c_{\rm eff}^2$ decreases the amplitude of fluctuations in the matter relative to the potential fluctuations. On the other hand, as we shall see in the next section, decreasing $c_{\rm eff}^2$ also eliminates a source of CMB anisotropies such that the *COBE* signal drops relative to the potential fluctuations. These two effects compete such that the change in normalization of $P(k)$ at large scales with $c_{\rm eff}^2$ is nonmonotonic. The shape of the power spectrum above and below the transition region of equation (20) remains that of a CDM model with the same $\Omega_m h$ and $\Omega_b h^2$ (see σ_{50}/σ_8 in Fig. 4).

4.2. *Viscous Scale and Radiation*

As discussed in § 3.3, the effect of changing the viscous scale through $c_{\rm vis}^2$ has little effect on the spectrum of matter fluctuations as long as $|c_{\rm eff}^2| > |c_{\rm vis}^2|$. We show an example in Figure 5*a* where the neutrinos in sCDM have been replaced with GDM as in Figure 3. In the large-scale structure regime, the difference between these models and sCDM is small and $c_{\rm vis}^2 = \frac{1}{3}$ in particular provides an excellent approximation to free-streaming neutrinos.

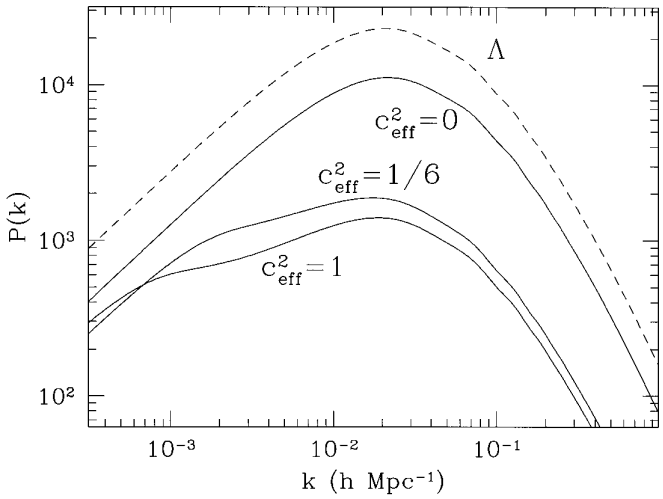

FIG. 4.—The effective sound horizon and the *COBE* normalized matter power spectrum. Raising $c_{\rm eff}^2$ from 0 to 1 (*solid lines*) introduces a feature between the effective sound horizon at GDM domination and that scale today. Here $\sigma_8 = (0.75, 0.29, 0.25)$ and $\sigma_{50}/\sigma_8 = (0.16, 0.17, 0.16)$ for $c_{\rm eff}^2 = (0, \frac{1}{6}, 1)$. These models have $w_g = -\frac{1}{6}$, $c_{\rm vis}^2 = 0$, $\Omega_{\rm tot} = 1$, $\Omega_g = 0.65$, $\Omega_b h^2 = 0.0125$, $h = 0.7$, and tilt $n = 1$. For comparison, the corresponding Λ model ($w_g \to -1$, same parameters; $\sigma_8 = 1.1$, $\sigma_{50}/\sigma_8 = 0.16$; *dashed lines*), which fits the current large-scale structure data, is also shown.

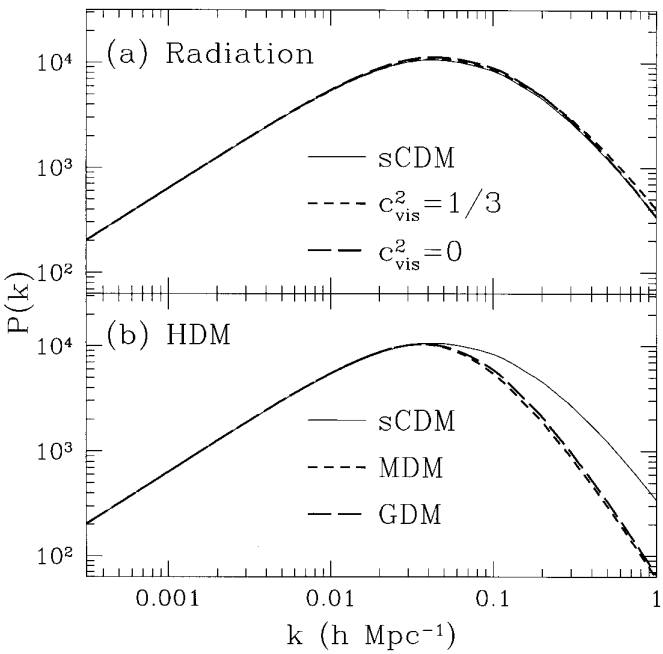

FIG. 5.—(*a*) Modeling radiation. Shown here is the power spectrum for the model of Fig. 3 where GDM of $w_g = \frac{1}{3}$ replaces the neutrinos of sCDM. Altering the viscosity parameter from $c_{\rm vis}^2 = \frac{1}{3}$ to 0 has little effect on the power spectrum although $\frac{1}{3}$ is a somewhat better approximation at large scales. (*b*) Modeling HDM. The features of the mixed dark matter are well reproduced by GDM with the same equation of state and $c_{\rm vis}^2 = w_g$. The parameters here are sCDM with $\Omega_\nu = 0.2$ replacing part of the CDM.

4.3. *Time-Dependent Stresses and MDM*

In general, the stress parameters (w_g, $c^2_{\rm eff}$, $c^2_{\rm vis}$) may all be time dependent. An interesting concrete example of such a model is provided by the mixed dark matter (MDM) scenario where a component of HDM (e.g., massive neutrinos) is added to the CDM. Here the equation of state goes from $w_{\rm hdm} = \frac{1}{3}$ to 0 as the neutrinos become nonrelativistic. Fitting to the numerical integration of the distribution gives

$$w_{\rm hdm} = \tfrac{1}{3}[1 + (a/a_{\rm nr})^{2p}]^{-1/p}\,, \tag{21}$$

with $p = 0.872$ and $a_{\rm nr} = 6.32 \times 10^{-6}/\Omega_\nu h^2$. We can model its behavior as a GDM component with $w_g = w_{\rm hdm}$, $c^2_{\rm eff} = c^2_g$ given by equation (4), and $c^2_{\rm vis} = w_{\rm hdm}$. In Figure 5*b* we show that this model accurately reproduces the features of the MDM model as calculated by CMBFAST (Seljak & Zaldarriaga 1996). The novelty of this type of model is that the ratio of the clustering scale to the horizon scale varies, in this case shrinking with time. This can have the effect of smoothing out the clustering feature in the matter-power spectrum (see Figs. 4 and 5*b*).

An exotic example of this type of model is the self-interacting dark matter candidate proposed by Carlson, Machacek, & Hall (1992), where the equation of state passes through a logarithmically decaying regime

$$w_g = \frac{1}{3\ln(a/\bar{a})}\,, \tag{22}$$

between the radiation and matter limits of $w_g = \frac{1}{3}$ and $w_g \propto a^{-2}$. Here $\bar{a}$ is a constant.

Other examples include a scalar field that rolls from a potential dominated regime with $w_g = -1$ to a kinetic energy dominated regime with $w_g = 1$ (decaying-Λ scenarios, see, e.g., Coble et al. 1997). The scalar field may also go from a rolling to a rapidly oscillating regime where sub-horizon clustering can take place. Here one must redefine $c^2_{\rm eff}$ to be time variable as well. This may occur in certain two-field models where the mass term can be time dependent (see the Appendix).

4.4. *GDM-Only Models*

The freedom to set the clustering scale well below the horizon ($c^2_{\rm eff} \ll 1$) raises the possibility that there is only a single component of dark matter with $w_g < 0$, i.e., CDM is absent. Conventional scalar field models (e.g., Caldwell et al. 1998) do not allow this possibility, since perturbations could never grow beyond the small amplitude they possessed at horizon crossing (but see the Appendix).

The lack of a CDM component allows the appearance of interesting phenomena in the matter-power spectrum. The main effect is that the shape parameter of CDM is rescaled for a given $\Gamma = \Omega_g\, h$, because the relevant scale is the horizon at GDM-radiation equality given by equation (19), i.e.,

$$\frac{\Gamma_{\rm eff}}{\Gamma} = \left(\frac{\Omega_r}{\Omega_g}\right)^{-3w_g/(1-3w_g)}\,, \tag{23}$$

where $\Omega_r = 4.17 \times 10^{-5} h^{-2}$ with the usual thermal history. Note that w_g appears in the exponent for the shape parameter $\Gamma_{\rm eff}$ and hence even a mild departure from zero yields dramatic effects. In Figure 6*a* we show an example with $w_g = -0.04$ GDM replacing the CDM in a model with $\Omega_{\rm tot} = 1$, $h = 0.65$, $\Omega_b h^2 = 0.0125$, and $n = 1$ (*solid lines*). This model has $\Gamma_{\rm eff} = 0.24$ and closely resembles a CDM model with $\Gamma = \Omega_m h = 0.24$ (*short-dashed lines*). Not only does lowering w_g from zero help the problems of the normalization and shape of the CDM power spectrum, it also raises the age.

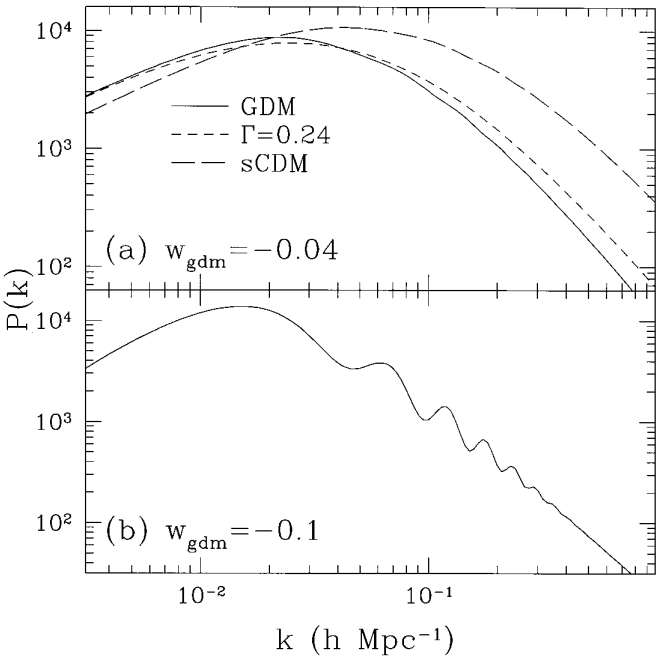

FIG. 6.—GDM-only Models. (*a*) $w_g = -0.04$. Here an $h = 0.65$ model with otherwise sCDM parameters is shown (*solid line*; $\sigma_8 = 0.60$, $\sigma_{50}/\sigma_8 = 0.17$) in comparison with sCDM (*long-dashed line*) and a CDM model with $\Gamma = \Omega_m h = 0.24$ (*short-dashed line*) with a normalization artificially set to match the GDM model. (*b*) $w_g = -0.1$. Acoustic features appear even though the model is a critical universe ($\Omega_{\rm tot} = 1$, $h = 0.65$) with big bang nucleosynthesis baryons ($\Omega_b h^2 = 0.025$). The suppression of GDM power is counteracted by a strong blue tilt $n = 1.7$ ($\sigma_8 = 0.40$, $\sigma_{50}/\sigma_8 = 0.23$).

Of course, the small change from $w_g = 0$ to -0.04 in the example above only increases the age from to a negligible amount from 10 to 10.4 Gyrs ($h = 0.65$). If we push w_g to -0.1, the age is 11.1 Gyrs, but $\Gamma_{\rm eff}$ is too small to account for large-scale structure with a scale-invariant $n = 1$ spectrum. This sort of model can be made viable by blue-tilting the initial spectrum. In Figure 6*b* we show an example with $\Omega_{\rm tot} = 1$, $h = 0.65$, $\Omega_b h^2 = 0.025$, and $n = 1.7$ (with a *COBE* normalization to a model with reionization at $z = 65$ in order that the large tilt be consistent with degree-scale anisotropies). It is interesting to note that the GDM power is so suppressed that even with this big bang nucleosynthesis baryon content, acoustic oscillations are visible in a critical density model. In fact, there is an interesting feature in this model at the 100 h^{-1} Mpc scale of $k \sim 0.05$–$0.07\ h$ Mpc^{-1}. These models thus escape the constraints presented in Eisenstein et al. (1997) and may help to explain the observed 100 h^{-1} Mpc excess should it persist. More generally, the replacement of CDM with $w_g < 0$ GDM gives one the freedom to increase the prominence of the acoustic oscillations in the matter-power spectrum.

5. CMB ANISOTROPIES

The presence of GDM affects the CMB anisotropies both by its influence on the background expansion (§ 5.1) and on the gravitational potential perturbations (§ 5.2). If $w_g < 0$ and CDM is also present, small-angle anisotropies are affected only by the former since the perturbations that

generated them entered the horizon when the GDM effects were negligible. We discuss the case where it is absent below in § 5.3. Large-angle anisotropies depend mainly on gravitational potential variations (the integrated Sachs Wolfe [ISW] effect), since primary anisotropies have few features that can be shifted by a change in the background geometry.

5.1. *Acoustic Peaks*

The acoustic peaks in the CMB depend on the photon to baryon ratio, the expansion rate at last scattering, and the gravitational potential, all at last scattering, as well as the angular diameter distance to last scattering (Hu & White 1996). Provided that GDM contributes negligibly to the density at last scattering, it can only alter the peaks through the last effect. Here features shift in scale with the angular diameter distance, which in a flat universe is

$$d_A = \eta_0 - \eta_* \,. \tag{24}$$

Here $\eta_* \equiv \eta(a_*)$ is the conformal time at last scattering (see Hu & White 1997a, eqs. [22]–[23]). We display this effect in Figure 7, where the angular scale of four models with $-1 \le w_g \le -\frac{1}{6}$ is rescaled via the d_A of a fiducial $w_g = -1$ model. As w_g decreases, d_A increases such that features are shifted to smaller angular scales.

5.2. *ISW Effect*

A more complicated effect arises from the decay in the gravitational potential induced by the GDM. This is called the late ISW effect and produces a contribution to C_ℓ as

$$C_\ell^{(\mathrm{ISW})} = \frac{2}{\pi}\int \frac{dk}{k}\, k^3 \left\{\int_{\eta_*}^{\eta_0} d\eta (\dot{\Psi} - \dot{\Phi}) j_\ell[k(\eta_0 - \eta)]\right\}^2 , \tag{25}$$

which appears at large angles. On small scales, the photons can traverse many wavelengths of the fluctuation during the decay time and thus destroy the coherence of the gravitational redshifts. The cancellation is expressed by the integral over the oscillatory Bessel function.

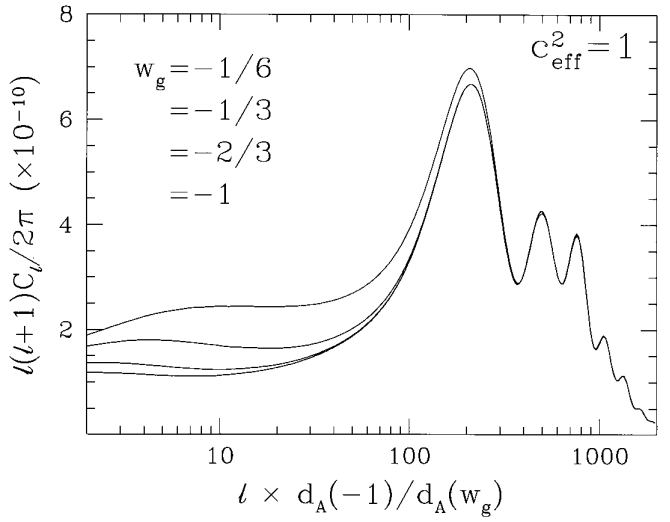

FIG. 7.—Angular diameter distance, the acoustic peaks, and the late ISW effect. Small-angle anisotropies depend on the equation of state w_g through the angular diameter distance d_A. Once the angular scale is rescaled to the fiducial d_A of a $w_g = -1$ (Λ) model, the curves are indistinguishable if normalized to small scales. Large-angle contributions arise from the ISW effect and are maximal in these scalar field $c^2_{\mathrm{eff}} = 1$ examples. Here $\Omega_{\mathrm{tot}} = 1$, $\Omega_g = 0.65$, $h = 0.7$, and $\Omega_b h^2 = 0.0125$.

The effect is minimized if $c_{\mathrm{eff}} \ll 1$. A concrete example of this is the MDM scenario where the hot component has $w_g = 0$ and an effective sound horizon today well below the particle horizon. Hence there is essentially no ISW contribution in this model (see Fig. 9). More generally, there will be a small effect if $w_g \neq 0$ because of the mild potential variation from the change in the equation of state (see eq. [14]).

The effect is maximized for $c_{\mathrm{eff}} = 1$, as is the case for scalar field models shown in Figure 7. Here the potential decays due to pressure support of the GDM fluctuations during GDM domination. The crucial aspect is that the decay occurs as soon as the perturbation crosses the horizon so that the photons have not had sufficient time to cross the perturbation. The effect thus monotonically decreases as c^2_{eff} decreases to zero. In Figure 8, we display this trend in C_ℓ. Here we properly normalize the spectrum to the *COBE* detection, which corresponds roughly to $\ell = 10$. Thus as c^2_{eff} increases, the height of the acoustic peaks decreases relative to the ISW-boosted large-scale anisotropy. This also has the consequence of decreasing the normalization of the matter-power spectrum as we have seen in Figure 4.

5.3. *Special Cases*

It is worthwhile to consider a few special cases to further illustrate the range of phenomena and show how more conventional candidates are recovered. As we have seen in § 3.3, radiation can be modeled through the viscous parameter c^2_{vis}. Changing c^2_{vis} has a greater effect on the CMB than on the matter-power spectrum, since it enters directly into the evolution of the gravitational potentials (see eq. [13]). In Figure 9*a* we show the model of Figures 3 and 5*a*, where the neutrinos in sCDM are replaced by GDM of $w_g = c^2_{\mathrm{eff}} = \frac{1}{3}$. The model with $c^2_{\mathrm{vis}} = \frac{1}{3}$ yields an excellent approximation to the neutrinos, whereas that with $c^2_{\mathrm{vis}} = 0$ differs by $\sim 20\%$ from the sCDM results (see also Hu et al. 1995).

Likewise the GDM model for a hot component presented in § 4.3 accurately reproduces the anisotropies of an MDM model (see Fig. 9*b*). Note that this model has essentially no late ISW effect and differs from sCDM (*long-dashed lines*)

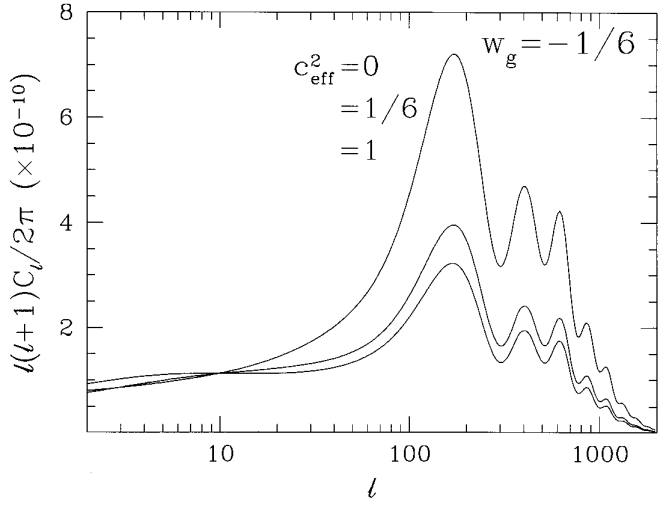

FIG. 8.—Sound speed effects. Decreasing c^2_{eff}, for a fixed background cosmology with $w_g = -\frac{1}{6}$ and the same cosmological parameters as Fig. 7, decreases the ISW effect at large angles such that *COBE* normalized models have lower acoustic peaks.

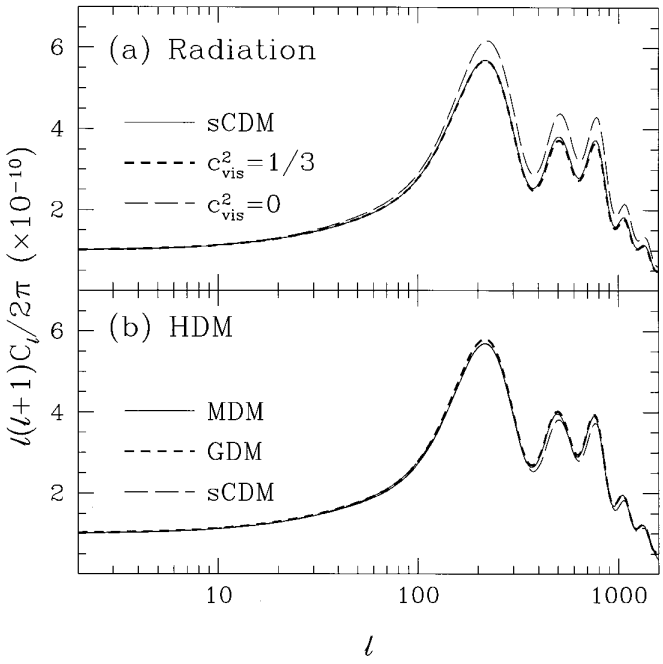

FIG. 9.—(*a*) Modeling radiation. Shown here are the anisotropies for the model where the neutrinos of sCDM are replaced with GDM $w_g = \frac{1}{3}$ as in Fig. 5*a*. Changing the viscosity parameter alters the anisotropies with $c^2_{vis} = \frac{1}{3}$ best approximating the neutrinos. (*b*) Modeling HDM (same parameters as Fig. 5*b*). The GDM model accurately reproduces the features of MDM that are themselves only slightly different from sCDM.

only through the small change in the expansion rate and gravitational potentials due to the presence of the hot component at last scattering. MDM models have larger small-scale anisotropies due potential decay from the radiation pressure of the hot component (Ma & Bertschinger 1995; Dodelson, Gates, & Stebbins 1996). These results, in conjunction with the analogous ones for the matter-power spectrum presented in Figure 5, demonstrate that the GDM *Ansatz* also allows one to model the full range of leading particle dark matter candidates.

Finally, we show the CMB anisotropies for the single dark matter component model of Figure 6*a* in Figure 10.

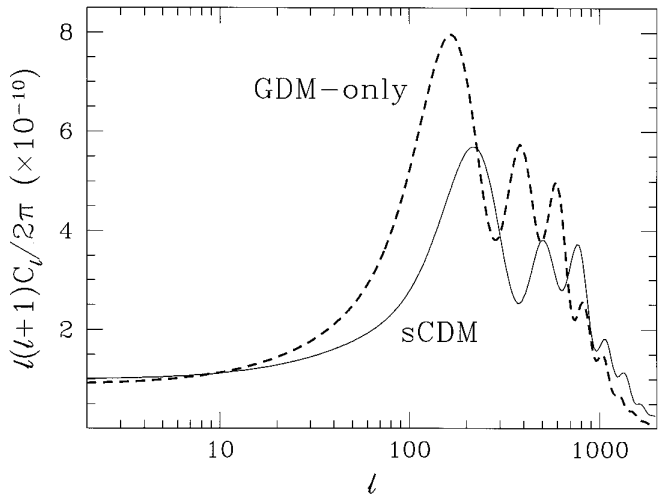

FIG. 10.—A GDM-only Model. CDM is replaced with GDM of $w_g = -0.04$ ($c^2_{eff} = c^2_{vis} = 0$) as in the model of Fig. 6*a*. Compared with the sCDM model, the acoustic peaks are of higher amplitude and larger angle as discussed in the text.

Models of this type tend to have enhanced degree-scale anisotropies. Because radiation domination is extended, there is more decay in the gravitational potentials due to radiation pressure support. This leads to early ISW contributions around GDM-radiation equality. Furthermore, the sound horizon at last scattering increases due to the extended period of radiation domination. This moves the acoustic peaks to slightly larger angles.

6. CONCLUSIONS

We have introduced a parameterization of a GDM component based on three quantities that can vary in time but not in space. These are the equation of state w_g, the effective sound speed c^2_{eff}, and the viscosity parameter c^2_{vis}. Combinations of these parameters recover all currently popular candidates for dark matter either exactly or to high accuracy, e.g., CDM, radiation, HDM, and scalar fields. Note that the computational costs of modeling the HDM is the same as CDM, which is in sharp contrast to a full solution to the energy-dependent Boltzmann equation for massive neutrinos (Ma & Bertschinger 1995).

In this general study, we have shown how the clustering scale of the GDM is not, in general, specified by its equation of state. The clustering scale appears as a feature in the matter-power spectrum but only a weak enhancement of CMB anisotropies at large angles. In fact, the contribution is bounded by the scalar field case of $c^2_{eff} = 1$ for any given equation of state. There exists a class of models where GDM clustering has dramatic effects on large-scale structure but no effect on the CMB (within cosmic variance). Conversely, altering the viscosity parameter of the dark matter affects the CMB anisotropies more strongly than the matter spectrum. An example of this behavior is provided by massless neutrinos. The difference between massless neutrinos and a perfect fluid with $w_g = \frac{1}{3}$ produces an observable difference in the CMB anisotropy spectrum. Finally, models exist where only a single species of dark matter is necessary in contrast to scalar field and MDM models where a comparable amount of CDM must also be present to form structure.

While observations currently do not force one to consider the exotic types of dark matter studied here, this situation may soon change with the high-precision measurements expected from the Microwave Anisotropy Probe on the CMB side and the 2 Degree Field and Sloan Digital Sky Survey on the galaxy-survey side (Hu et al. 1998a). The freedom to alter large-scale structure in relation to the CMB uncovered here may then be essential in the reconstruction of the cosmological model. This is especially true since the ambiguity introduced by the initial spectrum of fluctuations is removed once the CMB and large-scale structure are measured at the same physical scale. Here we have exposed the aspects of the dark matter to which the CMB and large-scale structure are and are not sensitive. These phenomenological aspects, once observationally determined, should aid in the isolation of a viable physical candidate for the dark matter.

I thank M. White for allowing me to modify his Boltzmann code for this work as well as D. J. Eisenstein and D. N. Spergel for useful discussions. This work was supported by the W. M. Keck Foundation and NSF PHY-9513835.

APPENDIX

SCALAR FIELDS AS GDM

In this appendix we demonstrate that scalar fields are recovered exactly as a limiting case of the GDM *Ansatz* and discuss a few special cases. A minimally coupled scalar field φ with the Lagrangian

$$\mathscr{L} = -\tfrac{1}{2}\sqrt{-g}\,[g^{\mu\nu}\partial_\mu\varphi\partial_\nu\varphi + 2V(\varphi)] \tag{A1}$$

and small perturbations, $\varphi = \phi_0 + \phi_1$ obeys

$$\ddot{\phi}_0 + 2\,\frac{\dot{a}}{a}\,\dot{\phi}_0 + a^2 V_{,\varphi} = 0 \tag{A2}$$

for the background field and

$$\ddot{\phi}_1 = -2\,\frac{\dot{a}}{a}\,\dot{\phi}_1 - (k^2 + a^2 V_{,\varphi\varphi})\phi_1 + (\dot{h}_v - 3\dot{h}_\delta)\dot{\phi}_0 - 2a^2 V_{,\varphi}\,h_v \tag{A3}$$

for the perturbations. Recall that the metric perturbations h_v and h_δ were defined for the synchronous and Newtonian gauges in equation (7).

From the stress-energy tensor

$$T^\mu_\nu = \varphi^{;\mu}\varphi_{;\nu} - \tfrac{1}{2}(\varphi^{;\alpha}\varphi_{;\alpha} + 2V)\delta^\mu_\nu\,, \tag{A4}$$

we can associate

$$\rho_\phi = \tfrac{1}{2}a^{-2}\dot{\phi}_0^2 + V\,, \qquad p_\phi = \tfrac{1}{2}a^{-2}\dot{\phi}_0^2 - V \tag{A5}$$

for the background and

$$\begin{aligned} \delta\rho_\phi &= a^{-2}(\dot{\phi}_0\,\dot{\phi}_1 - \dot{\phi}_0^2\,h_v) + V_{,\varphi}\,\phi_1\,, \\ \delta p_\phi &= \delta\rho_\phi - 2V_{,\varphi}\,\phi_1\,, \\ (\rho_\phi + p_\phi)v_\phi &= a^{-2}k\dot{\phi}_0\,\phi_1\,, \\ p_\phi\,\pi_\phi &= 0 \end{aligned} \tag{A6}$$

for the perturbations. The equations of motion can now be rewritten as

$$\dot{\rho}_\phi = -3(\rho_\phi + p_\phi)\,\frac{\dot{a}}{a} \tag{A7}$$

for the background and

$$\begin{aligned} \frac{d(\delta\rho_\phi)}{d\eta} &= -(\rho_\phi + p_\phi)(kv_\phi + 3\dot{h}_\delta) - \frac{\dot{a}}{a}\left[6\,\delta\rho_\phi + 9\,\frac{\dot{a}}{a}(1 - c_\phi^2)(\rho_\phi + p_\phi)\,\frac{v_\phi}{k}\right], \\ \frac{d[(\rho_\phi + p_\phi)(v_\phi/k)]}{d\eta} &= -\,\frac{\dot{a}}{a}\,(1 + 3c_\phi^2)(\rho_\phi + p_\phi)\,\frac{v_\phi}{k} + \delta\rho_\phi + (\rho_\phi + p_\phi)h_v\,. \end{aligned} \tag{A8}$$

One can rewrite the equations (1), (5), and (6) for the GDM as

$$\begin{aligned} \frac{d(\delta\rho_g)}{d\eta} &= -\,(\rho_g + p_g)(kv_g + 3\dot{h}_\delta) - 3\,\frac{\dot{a}}{a}\,p_g\,\Gamma_g - 3(1 + c_g^2)\,\frac{\dot{a}}{a}\,\delta\rho_g\,, \\ \frac{d[(\rho_g + p_g)(v_g/k)]}{d\eta} &= -4\,\frac{\dot{a}}{a}\,(\rho_g + p_g)\,\frac{v_g}{k} + c_g^2\,\delta\rho_g + p_g\,\Gamma_g - \frac{2}{3}\,(1 - 3K/k^2)p_g\,\pi_g + (\rho_\phi + p_\phi)h_v\,. \end{aligned} \tag{A9}$$

Employing equations (8) and (12), we find that GDM with $w_g = p_\phi/\rho_\phi$, $c^2_{\rm eff} = 1$, and $c^2_{\rm vis} = 0$ corresponds to a scalar field component.

Although exact, there are a few novel aspects concerning scalar fields that are hidden in this representation. The equation of state w_g encodes the potential V but is *not* completely specified by it. The equation of state is also dependent on how the field rolls in the potential as a function of time and this is dependent on the expansion rate, which acts a frictional term in equation (A2). This fact allows for novel features such as the attractor solutions investigated by Ferreira & Joyce (1997).

Furthermore, quadratic potentials $V = \frac{1}{2}m^2\varphi^2$, such as those found in axion models, cause the field and so the equation of state to rapidly oscillate. Here equation (A3) acts as a driven oscillator such that the perturbation does not stabilize until (Khlopov, Malomed, & Zeldovich 1985; Nambu & Sasaki 1990)

$$k^2 \gtrsim m\sqrt{G\rho_g}\,, \tag{A10}$$

despite the fact that $c_{\rm eff}^2 = 1$. Although the GDM description of equation (A9) formally holds, it is impractical to solve because of the widely separated expansion and oscillation timescales. One can, however, model this system by time averaging the oscillations and setting $w_g = 0$ and $c_{\rm eff}^2 \ll 1$ as is commonly done for axion models.

The field may be both rapidly oscillating and slowly rolling in certain two-field models (see, e.g., Kodama & Sasaki 1984 for multifield modifications to the equations of motion). Since the field evolution depends only on potential derivatives, the axion-type instability exists on short time scales. Nevertheless, on the expansion timescale the rolling contributes to the background density and pressure. Models of this type can have a net $w_g < 0$ but can cluster well below the horizon scale.

REFERENCES

Bardeen, J. M. 1980, Phys. Rev. D, 22, 1882
Bunn, E. F., & White, M. 1997, ApJ, 480, 6
Caldwell, R. R., Dave, R., Steinhardt, P. J. 1998, Phys. Rev. Lett., 80, 1582
Caldwell, R. R., & Steinhardt, P. J. 1998, Phys. Rev. D, 57, 6057
Carlson, E. D., Machacek, M. E., & Hall, L. J. 1992, ApJ, 398, 43
Chiba, T., Sugiyama, N., & Nakamura, T. 1997, MNRAS, 289, 5
Coble, K., Dodelson, S., & Frieman, J. 1997, Phys. Rev. D, 55, 1851
Dodelson, S., Gates, E., & Stebbins, A. 1996, ApJ, 467, 10
Eisenstein, D. J., Hu, W., Silk, J., & Szalay, A. S. 1998, ApJ, 494, L1
Ferreira, P. G., & Joyce, M. 1997, Phys. Rev. Lett., 79, 4740
Hu, W., & Eisenstein, D. J. 1998, in preparation
Hu, W., Eisenstein, D. J., Tegmark, M., & White, M. 1998a, preprint (astro-ph/9806362)
Hu, W., Scott, D., Sugiyama, N., & White, M. 1995, Phys. Rev. D, 52, 5498
Hu, W., Seljak, U., White, M., & Zaldarriaga, M. 1998b, Phys. Rev. D, 57, 3290
Hu, W., Spergel, D. N., White, M. 1997, Phys. Rev. D, 51, 3288
Hu, W., & White, M. 1996, ApJ, 471, 30
Hu, W., & White, M. 1997a, ApJ, 479, 568
———. 1997b, Phys. Rev. D, 56, 596
Jungman, G., Kamionkowski, M., Kosowsky, A., & Spergel, D. N. 1996, Phys. Rev. D, 54, 1332
Khlopov, M. Yu., Malomed, B. A., & Zeldovich, Ya. B. 1985, MNRAS, 215, 575
Kodama, H., & Sasaki, M. 1984, Prog. Theor. Phys. Supp., 78, 1
Ma, C.-P., & Bertschinger, E. 1995, ApJ, 455, 7
Nambu, Y., & Sasaki, M. 1990, Phys. Rev. D, 42, 3918
Peebles, P. J. E., Schramm, D. N., Kron, R. G., & Turner, E. L. 1991, Nature, 352, 769
Perlmutter, S. et al. 1998, Nature, 391, 51
Riess, A. G. et al. 1998, astro-ph/9805201
Seljak, U., & Zaldarriaga, M. 1996, ApJ, 469, 437
Spergel, D. N., & Pen, U.-L. 1997, ApJL, 491, L67
Turner, M. S., & White, M. 1997, Phys. Rev. D, 56, 4439
Turok, N., Pen, U.-L., & Seljak, U. 1997, Phys. Rev. D, 58, 023506